Breakthrough of stratospheric air masses into the upper troposphere retrieved from ozone lidar measurements

V.V. Zuev,[1] V.D. Burlakov,[1] S.I. Dolgii,[1] A.V. Nevzorov,[1] and A.V. El'nikov[2]

[1]Institute of Atmospheric Optics, Siberian Branch of the Russian Academy of Sciences, Tomsk
[2]Surgut State University

Received October 26, 2007

We present a technique for retrieving ozone concentration profiles via single-wavelength sensing under background aerosol conditions in the upper troposphere and lower stratosphere. At this wavelength, the radiation is considered, corresponding to first Stokes component of transformation of the Nd:YAG laser fourth harmonics (266 nm) in hydrogen (299 nm) on the base of the effect of stimulated Raman scattering. Ozone concentrations were measured in a height range 6–14 km. Based on results of lidar measurements of ozone and the data of aerological sensing of the temperature and humidity, a rather rare process of stratosphere–troposphere transfer through the tropopause was detected in April, 2007 above Tomsk (56.5°N; 85.0°E).

Introduction

Laser sensing of the ozone vertical distribution is conducted at the Siberian Lidar Station of the Institute of Atmospheric Optics (Tomsk, 56.5°N; 85.0°E) since 1989. The measurements are carried out by the method of differential absorption (DA) in the region of the Hartley–Huggins ozone absorption band at wavelengths of 308 nm (on-line) and 353 nm (off-line), which correspond to the generation frequency of an excimer XeCl laser and its first Stokes component of transformation in hydrogen on the base of the effect of stimulated Raman scattering (SRS). The absorption cross section of ozone σ at a wavelength of 308 nm is $1.4 \cdot 10^{-19}$ cm^2 and at $\lambda = 353$ nm σ is close to zero.

The obtained lidar signals at these wavelengths provide for the concentration sensitivity of the DA method sufficient to determine stratospheric ozone at heights of 12–35 km, i.e., in the layer with maximal ozone content, where its concentration is $(2.0–6.0) \cdot 10^{12}$ mol/cm^3. Below 12 km, where ozone concentration is less by several times, the value of the absorption coefficient $K = \sigma N$ (N is the ozone concentration) is not sufficient to detect with confidence the absorption of the sensing radiation by ozone against the background of random errors of a lidar signal.

At the same time, some urgent problems of atmospheric physics and chemistry, in particular, the stratosphere–troposphere exchange (STE), require measurements just in the domain of the tropopause (higher and lower). Variations of the vertical ozone distribution are considered here as a tracer of general interchange of air in the tropopause region. Such investigations are necessary for the study of irreversible downward ozone transfer from the stratosphere to the troposphere, the role of STE processes in the general circulation of the atmosphere, the STE influence on changes in chemical composition of air, which, in turn, has an effect on the balance of radiation flows in the troposphere and lower stratosphere.

In the present-day investigations, STE processes are considered as a part of general circulation of the whole atmosphere, as one of the objects of the global pattern of transfer and mixing of atmospheric gaseous components. The STE is an individual subject of study in the framework of the SPARC International Project on stratospheric processes and their role in climate. The European Project STACCATO studies the STE influence on changes in the climate, atmospheric transport, and oxidation capacity of the troposphere.[1] To obtain vertical profiles of ozone distribution in the troposphere–stratosphere, lidar measurement methods are also used.[2,3] The technique and first results of such measurements at the Siberian Lidar Station are considered in this paper.

1. Instrumentation for lidar measurements

To improve concentration sensitivity of lidar ozone measurements in the troposphere, it is necessary to shift the sensing wavelength (on-line) to the shorter-wavelength region (relative to $\lambda = 308$ nm) of the Hartley band, where the absorption cross section of ozone is larger. Such a shift was realized by the use of radiation of the Nd:YAG laser fourth harmonic ($\lambda = 266$ nm). The radiation was transformed in a hydrogen SRS-cell into radiation with $\lambda = 299$ nm (the first Stokes component of the SRS-transformation). This wavelength falls into the region of the ozone absorption band with the absorption cross section $\sigma_{299} = 4.4 \cdot 10^{-19}$ cm^2.

The Nd:YAG laser, model LS-2134 UT by LOTIS TII (Minsk, Belarus), is used as a source of

0235-6880/08/07 514-06 $02.00

sensing radiation generated at λ = 532 and 266 nm with a pulse repetition frequency of 15 Hz. The SRS-cell is made of a stainless steel tube with an internal diameter of 3 cm and a length of 1 m. The input and output windows are made of quartz KU. The pulse pumping energy at λ = 266 nm is equal to 60 mJ. The pump power density, necessary for obtaining the effect of SRS-transformation, is provided by a lens with a focal length of 80 cm, which is mounted ahead of the SRS-cell and focuses radiation to the cell center. The collimating lens is mounted back of the cell, confocally with the focusing lens. When the hydrogen pressure in the cell reaches two atmospheres at λ = 299 nm, a 20 mJ pulse energy of radiation is realized.

Optical lidar signals are detected by the receiving telescope made following the Newton scheme on the base of a mirror of 0.5 m in diameter. The HAMAMATSU R7207-01 photoelectron amplifiers (PHA) are used as radiation receivers. Detection is realized in the photon counting mode.

To estimate the contribution of the aerosol component into the lidar signal attenuation, the second wavelength equal to 532 nm was used in order to obtain the scattering ratio $R(H)$, which represents height variations of the aerosol scattering relative to the molecular scattering and is defined as the ratio of the sum of coefficients of back aerosol and molecular scattering to the latter one.

Since 1996, the background state of the stratospheric aerosol layer (SAL) with minimal aerosol content is observed due to a long period of the calm volcanic activity: the last powerful explosive eruption was in 1991 (Pinatubo). Measurements demonstrate that vertical variations of R are insignificant[4] for the observed background state of SAL, and R values themselves are close to 1. In the lower stratosphere they vary on the average from 1.05–1.1 in summer to 1.1–1.15 in winter, i.e., the contribution of the aerosol component into the total scattering makes 5–15% of the scattered molecular component, whereas under conditions of stratosphere perturbation by a powerful volcanic eruption, the aerosol component can several times exceed the molecular scattering in the upper troposphere–stratosphere.

Under background conditions of a long period of low volcanic activity and in the absence of clouds (what is necessary for lidar measurements), a rather stable aerosol content even in the upper troposphere is observed. Figure 1 presents the form of lidar signals recorded at λ =299 and 532 nm on April 12, 2007, by 25 000 laser pulses, and the profile $R(H)$ measured at λ = 532 nm, which reflects the height distribution of aerosol in the stratosphere–troposphere.

In a height range of 6–12 km, the contribution of the aerosol component into the back scattering accounts for 10–15% of the molecular component and decreases to 5% in the stratosphere. Besides, according to model representations and experimental data, the ratio of aerosol scattering to molecular scattering also decreases with the wavelength decrease.[5–7] This makes it possible to neglect the aerosol contribution into lidar signals and retrieve the ozone concentration from sensing data at a single wavelength (λ = 299 nm), applying model values for correction of the total molecular contribution.

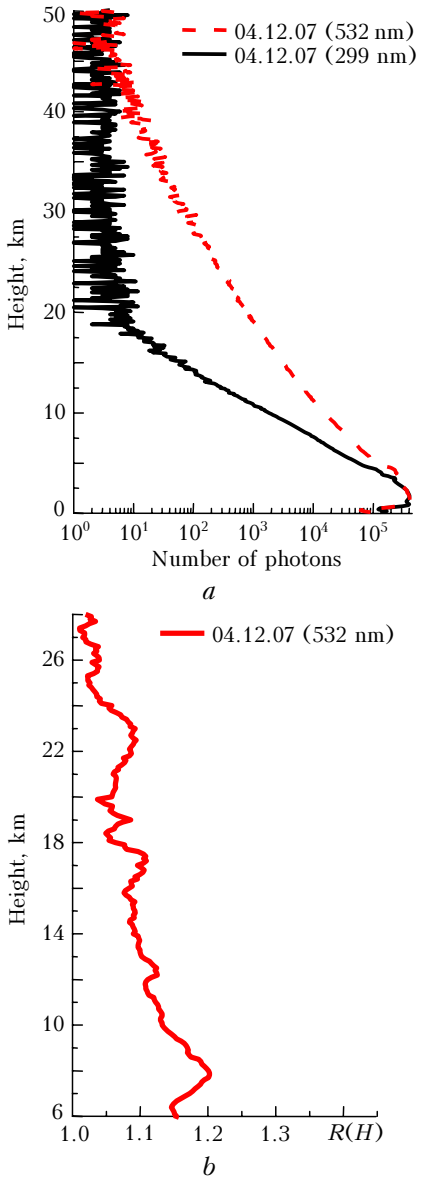

Fig. 1. Lidar signals at λ = 299 and 532 nm (April 12, 2007) (*a*); the retrieved profile of the scattering ratio at λ = = 532 nm (*b*).

The general form of the laser sensing equation in the presence of absorbing gas in the sensing path is as follows:

$$P(H) = \frac{C}{H^2}\left[\beta_\pi^a(H) + \beta_\pi^m(H)\right] \times$$

$$\times \exp\left[-2\int_0^H \left[\sigma N(h) + \alpha_m(h) + \alpha_a(h)\right] dh\right], \qquad (1)$$

where $P(H)$ is the power of the lidar signal; H is the height; C is the apparatus constant; $\beta_\pi^a(H)$ and $\beta_\pi^m(H)$

are coefficients of back aerosol and molecular scatterings; σ is the absorption cross section; $N(H)$ is the ozone concentration; $\alpha_m(h)$ and $\alpha_a(h)$ are coefficients of total molecular and aerosol scattering. With allowance for the assumption of small contribution of the aerosol component into the lidar signal under conditions of the background aerosol content in the stratosphere and upper troposphere, the equation (1) can be simplified:

$$P(H) = \frac{C}{H^2}\beta_\pi^m(H)\exp\left[-2\int_0^H\left[\sigma N(h) + \alpha_m(h)\right]dh\right]. \quad (2)$$

Let us regroup equation (2) and reduce it to the form

$$\exp\left[-2\int_0^H\left[\sigma N(h) + \alpha_m(h)\right]dh\right] = \frac{1}{C}\frac{S(H)}{\beta_\pi^m(H)}, \quad (3)$$

where $S(H) \equiv P(H)H^2$ is the so-called $S(H)$-function.

Further, we take the logarithm of Eq. (3) and resolve its right side into components:

$$-2\int_0^H\left[\sigma N(h) + \alpha_m(h)\right]dh =$$

$$= \ln\left(\frac{1}{C}\right) + \ln\left[S(H)\right] - \ln\left[\beta_\pi^m(H)\right], \quad (4)$$

differentiate it and, with allowance for the fact that the derivative of the constant is zero, obtain the expression for the doubled absorption coefficient:

$$2K(H) \equiv 2\sigma N(h) =$$

$$= \underbrace{-\frac{d}{dh}\ln\left[S(H)\right]}_{A} + \underbrace{\frac{d}{dh}\ln\left[\beta_\pi^m(H)\right]}_{B} - \underbrace{2\alpha_m(h)}_{C}. \quad (5)$$

Height distributions of absolute values of the summands "A" (in which the lidar signal accumulated for April 9, 2007 was used as the $S(H)$-function), "B", and "C" are presented in Figure 2.

Since "A" is a measured value, Figure 2 presents its random error as well. The bold line depicts the summand "A" after smoothing by a filter on the base of the fast Fourier transform over five points. The summands "A" and "B" were differentiated by the difference scheme. The apparatus spatial resolution of the measurements is equal to 100 m.

To increase absorption coefficients between neighboring points of the sensing path, four neighboring height intervals were united before the operation of numerical differentiation. This has led to spatial resolution of 400 m. As the result of numerical differentiation, which is known to be an ill-posed problem, the obtained vertical profile of ozone concentration has strong stochastic oscillations.

To decrease the oscillations, the filter based on the fast Fourier transform was used (as a module of the ORIGIN package). Five smoothing points were chosen, basing on two propositions: on the one hand, stochastic oscillations should not hide the vertical structure of the profiles; on the other hand, the spatial structure of the profile should be evident. Besides, the spatial filter of smoothing over five points decreases the random error to an admissible value in the height range of interest. This allows a conclusion about different vertical distributions of ozone concentration in the analyzed periods. Both winter and summer model values[5] were taken as $\beta_\pi^m(H)$ and $\alpha_m(h)$. In contrast to the summand "B", where the difference between seasons is still noticeable (although not higher than 5%), height behaviors for "C" are similar.

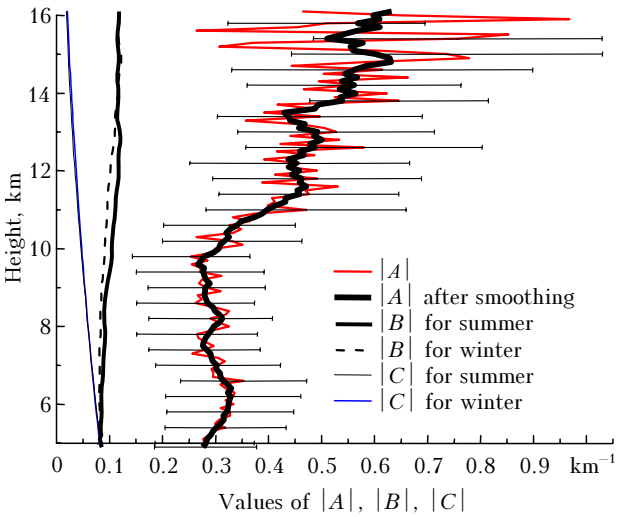

Fig. 2. Vertical distributions of absolute values of the summands $|A|$, $|B|$, and $|C|$ entering into equation (5).

In general, the analysis of information presented in Fig. 2, permits one to conclude that the arbitrariness in the choice of $\beta_\pi^m(H)$ and $\alpha_m(h)$ can introduce insignificant errors into the resulting ozone concentration, when a single wavelength (299 nm) is used.

The final expression, which is used further in calculation has the form

$$N(H) =$$

$$= \frac{1}{2\sigma}\left\{-\frac{d}{dh}\ln\left[S(H)\right] + \frac{d}{dh}\ln\left[\beta_\pi^m(H)\right] - 2\alpha_m(h)\right\}. \quad (6)$$

2. Results and analysis of lidar observations

The first measurements of ozone concentration in height range 6–14 km with the use of SRS-transformation of the Nd:YAG laser fourth harmonic were carried out in April, 2007. A sample of the obtained vertical ozone profiles is presented in Fig. 3 in comparison with the Krueger model.[9]

In height range 6–9 km, the empirical profiles and the model curve coincide sufficiently well. In the lower stratosphere above 9 km, some variability of the measured profiles (for April 6, 9, and 20) relative

to the model distribution is observed. This is natural for dynamics of the ozone distribution in individual days of observations. Beginning from 7 km and higher, the profile for April 12 differs from other profiles. The difference of its vertical behavior grows with height. On April 12 the ozone concentration was higher in the height range 7–13 km than in the previous and the next days of observations. This day, the relatively stable state of the ozonosphere in the region of the upper troposphere and lower stratosphere was broken by a short-time sporadic process, which caused an intrusion of stratospheric ozone masses into the troposphere.

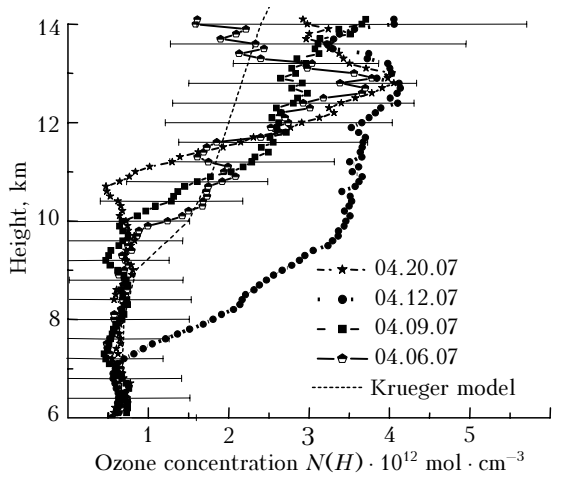

Fig. 3. Profiles of vertical ozone concentration measured in April, 2007 and the Krueger model.[9]

STE events in midlatitudes are connected with mesoscale processes and processes of the synoptic scale. The most favorable factors for transfer from stratosphere to troposphere are processes of air circulation in tropopause folds, at the cyclonic periphery of jet flows, in height troughs of pressure systems, within a circumpolar vortex, in cutoff cyclones, in mesoscale convective complexes and thunderstorms, during destruction of gravitation waves.[1] At the same time, STE are rapidly changing, discontinuous events separated by calmer periods. Temporal scales of STE processes can last for hours and days, spatial scales can be of hundreds and thousands of kilometers.[1,12]

One of the typical approaches to identifying and analyzing the process of stratosphere–troposphere transfer is studying the features of dynamics of the vertical ozone distribution, temperature, and humidity in tropopause.[1–3,12] The tropopause separates stratospheric and tropospheric air masses and, according to the World Meteorological Organization, is defined[10] as the lowest level, at which the temperature behavior decreases to 2 deg · km^{-1} or less, and the lapse rate between this level and any level within the next 2 km does not exceed 2 deg · km^{-1}.

A specific deformation of the tropopause can appear in baroclinic zones of the atmosphere, when the tropopause's surface inflects and takes an almost vertical position. This is the so-called tropopause fold. The features of circulation in the tropopause fold are considered as one of the main mechanisms of STE processes.[1] The descending movements can lead to adiabatic increase of temperature in troposphere and lower stratosphere. The decrease of relative humidity in the region of tropospheric heights, where the increase of ozone concentration is observed, indicates a descending transfer of stratospheric air masses with high ozone content and low humidity through tropopause into troposphere.

Since meteorological parameters are not sensed in Tomsk by aerology methods, we used the measurements of temperature and humidity profiles[8] obtained at the nearest to Tomsk sensing points: Kolpashevo (58.3°N; 83.0°E; 240 km from Tomsk) and Aleksandrovskoe (60.4°N; 77.9°E; 600 km from Tomsk) in the north-west direction; as well as Novosibirsk (55.0°N; 83.0°E; 220 km from Tomsk) in the south-west direction. The balloon measurements in days of lidar observations of ozone on April 6, 9, 12, and 20 were considered. Besides, the measurements obtained on April 12 were compared with those for the previous and the next days, on April 11 and 13. The balloon was launched at 12 GMT, which corresponded to 19.00 LT. This time is close to the average local time of ozone lidar measurements: 20.00–22.00.

Analysis of these data has shown that a typical height distribution of temperature with the pronounced tropopause was observed on April, 6, 9, 11, 13, and 20; as for April 12, the temperature distribution was almost vertical. Such a distribution was most pronounced for the northern stations Kolpashevo and Aleksandrovskoe. Figures 4 and 5 present data on temperature and humidity sensing at these stations.

As is seen in Figure 4, April 11 and 13 at the Kolpashevo station and April 13 at the Aleksandrovskoe station were characterized by the temperature distribution with a dip in the troposphere (6–7 deg · km^{-1}) and by a pronounced tropopause in the region of 10 km. However, already on April 13 at the Aleksandrovskoe station, distinct changes in vertical temperature variations began. The tropopause descended to 9 km, the fall of temperature at a height interval of 6–9 km was about 3 deg · km^{-1}. On April 12 in the height range 9–11 km the temperature distribution was observed, which was almost vertical in the tropopause fold, at which the tropopause is not a natural potential barrier for exchange of air masses between the stratosphere and troposphere. The fall of temperature in a height interval of 6–9 km was less than 2 deg · km^{-1} for both stations. Besides, at heights above 9 km the temperature was higher on April 12 than on April 11 and 13 at the Kolpashevo station, and at the Aleksandrovskoe station the temperature on April 11 and 12 was higher than on April 13. On the whole, the observed temperature variations in the region of anomalous ozone increase on April 12 correspond to the STE process. In a height interval 7–16 km, which includes the region of the ozone anomaly, the humidity (see Fig. 5) was lower on

April 12 as compared to the previous and next measurement days. This also points to the transfer of air masses from stratosphere to troposphere.

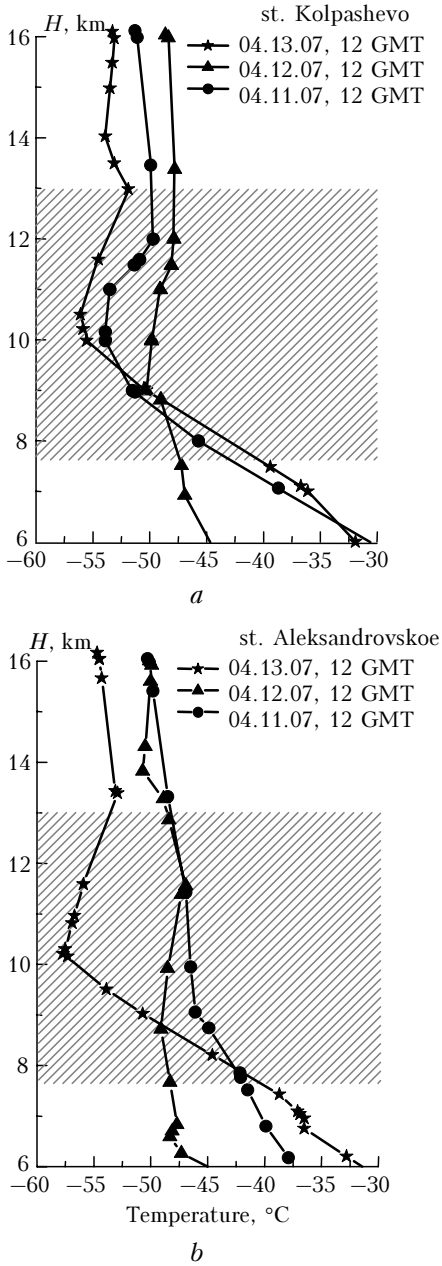

Fig. 4. Vertical profiles of temperature according to the data of the aerological stations in Kolpashevo (58.3°N; 83.0°E) (*a*) and Aleksandrovskoe (60.4°N; 77.9°E) (*b*). GMT is the balloon launch time. The hatched region shows the anomalous increase of ozone on April 12, 2007.

Besides, at the Aleksandrovskoe station, as in the case of temperature changes, a lower humidity was observed already on April 11 at 12.00 GMT, whereas at 00.00 GMT this day it was still higher.

In general, the combined observations of the ozone anomaly, temperature, and humidity demonstrate that the existence of the tropopause fold, as well as the stratosphere–troposphere transfer event itself are short-time processes, limited in this case not more than by 24 hours.

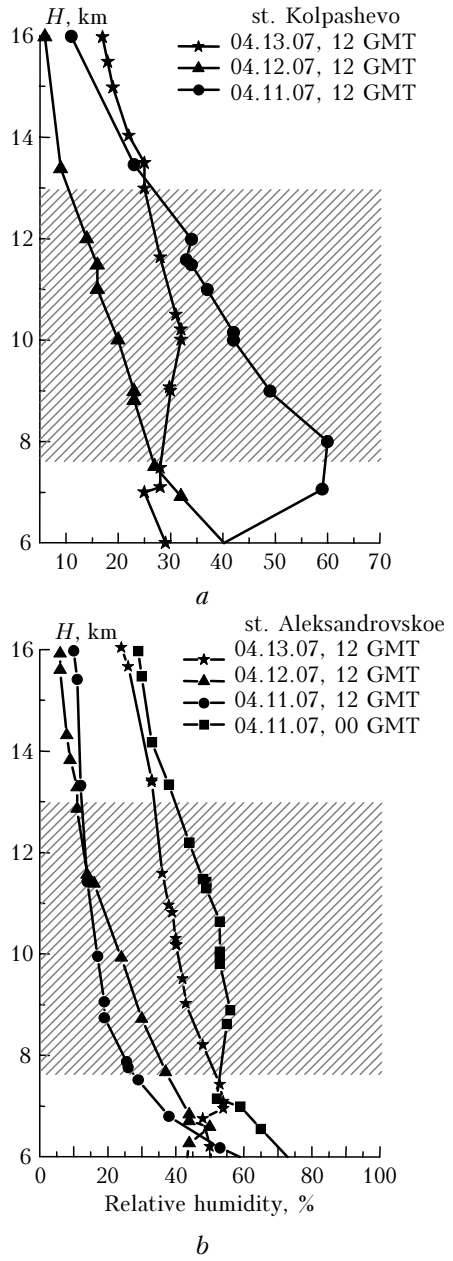

Fig. 5. Temporal behavior of the relative humidity according to the data of the Kolpashevo (*a*) and Aleksandrovskoe (*b*) aerological stations. GMT is the time of launching balloons. The hatched region corresponds to the anomalous increase of ozone on April 12, 2007.

The observed stratosphere–troposphere transfer could be connected with features of atmospheric circulation in April, 2007 over the Siberian region. The circulation was caused by a shift of the circumpolar vortex from the Barents Sea in the south-east direction.[11] Within the active zone of the circumpolar vortex, the descending transfer from the stratosphere to the troposphere is especially pronounced.[13] Most likely, variations in vertical distribution of the

temperature and humidity were observed at the northern station Aleksandrovskoe earlier than in Kolpashevo, in accordance with the direction of the circumpolar vortex motion. Observations of the STE events at the Tomsk station show that the tropopause fold manifested itself also above Tomsk and the temperature variations at the south-western station in Novosibirsk were weaker.

Conclusion

Results of lidar measurements of the vertical ozone distribution dynamics, conducted at the Siberian Lidar Station (at λ = 299 nm), together with data of aerological sensing of temperature and humidity have shown that a rather rare process of stratosphere – troposphere transfer was detected over Tomsk in April, 2007.

At present, the authors develop the technique and methods of ozone sensing in the upper troposphere and lower stratosphere by the method of differential absorption and scattering at two wavelengths of 299 and 341 nm, where 341 nm is the second harmonic of the SRS-transformation of the 266 nm line in hydrogen. This will make it possible to obtain information about vertical ozone distribution under any aerosol conditions.

Acknowledgements

This work was supported by the Federal Agency on Science and Innovations (Contract No. 02.518.11.7088), International Scientific-Technical Center (Project No. B-1063), Integration Project of the Siberian Branch of the Russian Academy of Sciences No. 3.14, and the Russian Foundation for Basic Research (Grant No. 05-05-64518).

References

1. A. Stohl, P. Bonasoni, P. Cristofanelli, and W. Collins, J. Geophys. Res. D **108**, No. 12, STA1/1–STA1/15 (2003).
2. E. Galani, D. Balis, P. Zanis, C. Zerefos, A. Papayannis, H. Wemli, and E. Gerasopoulos, J. Geophys. Res. D **108**, No. 12, STA12/1–STA12/10 (2003).
3. G.J. Roelofs, A.S. Kentarchos, T. Trickl, A. Stohl, W.J. Collins, R.A. Crowther, D. Hauglustaine, A. Klonecki, K.S. Law, M.G. Lawrence, R. von Kuhlmann, and M. van Weele, J. Geophys. Res. D **108**, No. 12, STA14/1–STA14/13 (2003).
4. V.V. Zuev, E. Burlakov, A.V. El'nikov, and A.V. Nevzorov, Atmos. Oceanic Opt. **19**, No. 7, 535–539 (2006).
5. I.I. Ippolitov, V.S. Komarov, and A.A. Mitsel', in: *Spectroscopic Methods of Atmosphere Sensing* (Nauka, Novosibirsk, 1985), pp. 4–44.
6. V.E. Zuev and G.M. Krekov, *Optical Models of the Atmosphere* (Gidrometeoizdat, Leningrad, 1986), 256 pp.
7. S.L. Bondarenko, A.V. El'nikov, and V.V. Zuev, Atmos. Oceanic Opt. **6**, No. 10, 727–732 (1993).
8. http://weather.uwyo.edu/upperair/sensing.html
9. A.J. Krueger and R.A. Minzner, J. Geophys. Res. D **81**, No. 24, 4477–4487 (1976).
10. World Meteorological Organization (WMO), Atmospheric Ozone 1985, WMO Global Ozone Res. and Monit. Proj. Rep. 20 (Geneva, 1986).
11. E.V. Vasil'ev, B.I. Luk'yanov, and M.G. Naishuller, Meteorol. Gidrol., No. 7, 113–118 (2007).
12. A.A. Kukoleva, Izv. Ros. Akad. Nauk, Ser. Fiz. Atmos. Okeana **38**, No. 5, 683–693 (2002).
13. C. Appenzeller, J.R. Holton, and K.H. Rosenlof, J. Geophys. Res. D **101**, No. 6, 15071–15078 (1996).